J. Int. Environmental Application & Science, Vol. 9(2): 194-204 (2014)

Adsorption of Lead Ions onto Cattle Bone

C. I. Egwuatu*, O. F. Obumselu, C. J. O.Anarado, N. L. Umedum,

Department of Pure and Industrial Chemistry, Nnamdi Azikiwe University, P. M. B. 5025 Awka, Anambra State, South Eastern Nigeria

Received December 14, 2013; Accepted June 06, 2014

Abstract: The sorption kinetics, thermodynamics and isotherms of lead adsorption on cattle bone were investigated. FTIR analysis revealed the presence of functional groups like OH^-, CONH, PO_4^{3-}, CO_3^{2-} that were capable of adsorbing Pb^{2+}. Results showed that the pseudo-second order kinetic model with R2 best described the kinetics, and $q_{theoritical}$ values of 0.9999 and 0.96955 mg/g. Equilibrium data were well described by both Freundlich and Langmuir isotherms with R^2 values of 0.9975 and 0.9967. Maximum sorption capacity q_{max} obtained was 1.9573mg/g. Optimum sorption was observed at pH 4. Thermodynamics parameters obtained were ΔH (91.237kJ/mol), ΔS (-0.293kJ/mol/K). ΔG values were positive, increasing with increase in temperature.

***Keywords**: lead ion, Adsorption, Isotherm, Kinetic studies, Thermodynamics,*

Introduction

Lead is a poisonous metal that can damage nervous connections (especially in young children) and cause brain disorders. Lead poisoning typically results from ingestion of food or water contaminated with lead; but may also occur after accidental ingestion of contaminated soil, dust, or lead based paint (http://www.pencils.com/pencil-history). Lead that is emitted into the atmosphere can be inhaled, or ingested after it settles out of the air. It is rapidly absorbed into the bloodstream and is believed to have adverse effects on the cardiovascular system, kidneys, and the immune system). In pregnant women, high levels of exposure to lead may cause miscarriage. Chronic, high-level exposures have been shown to reduce fertility in males (Golub, 2005). Sources of lead pollution include exhaust fumes from automobiles, wastewater from battery manufacturing, metallurgical, metal-finishing and chemical industries. Therefore searching for low-cost alternative methods for metal removal has become a challenge worldwide (AjayKumar, et al., 2009). Methods exist for the removal of toxic metal ions from aqueous solutions, such as ion exchange, chemical precipitation, and adsorption, *etc*. (Krikaet al., 2012; Sari & Tuzen, 2009). Among these methods, adsorption is by far the most versatile and widely used process (Vimala & Das, 2009; Pehlivan et al., 2008; Ghodbaneet al., 2008).

Bones are rigid organs that constitute part of the endoskeleton of vertebrates. They support and protect the various organs of the body; produce red and white blood cells and store minerals. Bone is a composite material consisting of a mineral phase (hydroxyapatite), collagen, noncollagenous proteins, lipids, and water) Boskey et al., 2007).

Bones from slaughtered animals have a number of uses. They have been used as crafting material for buttons, handles, ornaments etc. Ground bones are used an organic phosphorus-nitrogen fertilizer and as additive in animal feed. Bones, in particular after calcination to bone ash are used as source of calcium phosphate for the production of bone china and previously also phosphorus chemicals (Bertazzo & Bertran, 2006). Bone char derived from heating the animal bone to 500–600 ^oC could be used to remove fluoride from drinking water on a laboratory scale (Christoffersen et al., 1991; Larsen *et al*., 1993; Phantumvanit & LeGeros, 1997). In recent studies, bone char was used to adsorb the radioisotopes of antimony and europium ions from radioactive wastes (Bennett & Abram, 1967). In the past, cattle bones have been used for preparing bone char but recently a new biological sorbent prepared from animal bones heated at 80°C for 24 h has been utilized for the recovery of copper and nickel (Sameer *et al*., 1999). The present study investigates the kinetics, equilibrium and thermodynamics of lead adsorption onto cattle bone.

Materials and Method

* *Corresponding: E-Mail: chy4jesusalwayz@yahoo.com, Tel: +2348063620152;*

Preparation and Characterization of Adsorbent

Cattle bones were obtained from Kwata abattoir Awka, Eastern Nigeria. These were washed with distilled water and sun-dried for 48hrs. They were later ground to powder in a mill and sieved using a Particle Size Distribution analyser (Model 117.08, MALVERN instruments, USA), to obtain particle size of 350µm prior to use. For all the adsorption experiments, 3 g of ground bone sample were used in each case. Characterization of the adsorbents was carried out by FT-IR studies. FT-IR (FTIR RX-1, PerkinElmer, USA) spectrometer was employed to determine the functional groups in cattle bone responsible for metal adsorption. Atomic adsorption spectrophotometer (VARIAN SPECTRAAA55) was used to determine concentration of lead ion in standard and used solutions. The pH of the solutions was measured with a 5500 EUTECH pH meter using solid electrode calibrated with standard buffer solutions.

Preparation of Pb^{2+}standards

The stock solution containing 1000 mg/l of standard Pb^{2+} was prepared by dissolving 1.56g of AR grade $Pb(NO_3)_2$ in 200 ml of deionized water with few drops of H_2SO_4 added. The solution was then made up to 1000ml. Batch adsorption experiments were performed after proper dilution of the stock solution.

Adsorption Experiments

The uptake of Pb^{2+} as a function of H^+ ion concentration was determined in the pH range of 2–8. The adjustment of initial pH of solutions was carried out by adding required amount of dilute0.1 M NaOH and 0.1 M HCl solutions. 100ml of varying concentrations (10 mg/l, 20 mg/l, 30 mg/l, 40 mg/l, and 50mg/l) of the Pb^{2+} solution was introduced into conical flasks containing the 3 g of adsorbent. These were stirred mechanically and allowed to stand for 1hr while other parameters such as temperature, pH and time were kept constant. Samples were drawn out from the mixture and analyzed using AAS at working current/wavelength of 10mA/283.3 nm.

All the chemicals used in the study were of analytical grade and obtained from E. Merck Limited, Mumbai, India. The adsorption equilibrium data were conveniently represented by adsorption isotherms, which show the relationship between the mass of the solute adsorbed per unit mass of adsorbent q_e and the soluteconcentration C_e in the solution at equilibrium.

Batch kinetic experiments were performed using a mixture of 200 ml of 40 mg/l of Pb^{2+} solution and the adsorbent. Other parameters were kept constant while samples were drawn at time intervals of 5, 10, 30, 60, 90 and 120min and analyzed. The kinetics of Pb^{2+}adsorption on cattle bone was studied using pseudo-first-order, pseudo-second-order [Ho et al., 2001] and intra-particle diffusion [Weber and Morris, 1963] models. The conformity between experimental data and the model predicted values was expressed by the correlation coefficients (R^2).

Equation (1) represents the relation used for the determination of metal uptake q in (mg/g).

$$q = \frac{C_i - C_f}{m} V \quad \ldots\ldots\ldots\ldots\ldots\ldots\ldots\ldots 1$$

where C_i is initial metal concentration in mg/l, C_f final metal concentration in mg/l, m mass of adsorbent in g and V volume of solution in L

Data Analysis

Equilibrium Studies

The data obtained from experiment were fitted into four different isotherm models namely; Langmuir, Freundlich, Temkin and Dubnin-Radushkevich models. The correlationcoefficientsR^2 were also obtained to find the best fit adsorption isotherm model.

The Langmuir isotherm model

The Langmuir isotherm model is valid for monolayer adsorption [Langmuir, 1918] and is represented by the following linearized equation:

$$\frac{1}{q} = \frac{1}{q_{max} k_L C_e} + \frac{1}{q_{max}} \quad \ldots\ldots\ldots 2a$$

where q is the amount of adsorbed metal in mg/g, q_{max} is the maximum sorption capacity in mg/g, K_L is the Langmuir constant. A plot of 1/q v $1/C_e$ allows for the determination of q_{max} and k_L.
The essential characteristics and the feasibility of the Langmuir isotherm is expressed in terms of a dimensionless constant separation factor or equilibrium parameter R_L, which is defined as,

$$R_L = \frac{1}{1 + bC_0} \quad \ldots\ldots\ldots 2b$$

The R_L value indicates the shape of the isotherm as follows:

Table 1. R_L values and significance

R_L value	Type of isotherm
$R_L > 1$	Unfavourable
$R_L = 1$	Linear
$0 < R_L < 1$	Favourable
$R_L = 0$	Irreversible

The Freundlich isotherm model
The Freundlich isotherm is purely empirical and is based on adsorption on a heterogeneous surface [Freundlich, 2006]. The equation in linearized form is given as:

$$\ln q = \ln k_F + \frac{1}{n} \ln C \qquad 3$$

Where K_F is Freundlich constant. A plot of lnq vs. lnC is used to determine k_F and n.

Temkin isotherm model
The equation for the above model is given as;

$$q = \frac{RT}{b} \ln k_T + \frac{RT}{b} \ln C \qquad 4$$

q is amount adsorbed per gram of the adsorbent (mg/g), C is concentration of metal ion after certain period of time (mg/L), K_T and b are Temkin constants, R is universal gas constant (8.314J/K/mol) and T is temperature in Kelvin.
A plot of q vs. lnC will give a slope and an intercept from which b and k_T are evaluated (Mahamadi & Nharingo, 2010; Vijayaraghavan, et al., 2006).

Dubinin–Radushkevich isotherm (D-R) model
This isotherm assumes that the characteristics of the sorption curve are related to the porosity of the biosorbents (Abdelwahab et al., 2007). This model was chosen to evaluate the mean energy of sorption. It is represented in the linear form by the equation (Igwe & Abia, 2007).

$$\ln q = \ln q_m - \beta\varepsilon^2 \qquad 5$$

Where

$$\varepsilon = RT \ln\left(1 + \frac{1}{C_e}\right) \qquad 6$$

where q is amount adsorbed per gram of the adsorbent (mg/g),q_m is equilibrium adsorption capacity (mg/g) using model, β is Polanyi potential, ε is activity coefficient, C_e is concentration of metal ion in solution at equilibrium (mg/L), R is universal gas constant (8.314J/K/mol) and T is temperature in Kelvin.
The values ofβ and q_m are evaluated from the slope and intercept of the graph of lnq versus ε^2. The mean energy of sorption E (kJ mol^{-1}) is calculated from the relation [Horsfall Jr et al (2004)]

$$E = \frac{1}{\sqrt{2\beta}} \qquad 7$$

Kinetic Studies

Lagergren model

The pseudo-first-order kinetic model was proposed by Lagergren. Its integral form of is expressed as follows:

$$q_t = q_e\left(1 - e^{-k_1 t}\right) \ldots\ldots\ldots\ldots 8a$$

Linearizing equation 8a yields

$$Ln\left(q_{e(expt)} - q_t\right) = Lnq_{e(theo)} - k_1 t \quad 8b$$

Where $q_{e\ (expt)}$ and $q_{e\ (theo)}$ are the experimental and theoretical equilibrium adsorption and q_t is experimental amount of metal ion adsorbed (mg/g of adsorbent) at any time t(min)

Pseudo-second-order model

The kinetics of adsorption process was also described by the pseudo-second-order rate equation expressed by [Ho and McKay, 1999] as

$$\frac{dq}{dt} = k_2\left(q_{e(theo)} - q_t\right)^2 \ldots\ldots\ldots\ldots\ldots\ldots\ldots\ldots\ldots\ldots\ldots\ldots 9a$$

Separating the variables in Equation 9a gives;

$$\frac{dq}{\left(q_{e(theo)} - q_t\right)^2} = k_2\, dt \ldots\ldots\ldots\ldots\ldots\ldots\ldots\ldots\ldots\ldots\ldots\ldots\ldots\ldots 9b$$

Integrating Equation 9b for the boundary conditions t_0 to t_t and q_0 and $q_{e(theo)}$gives

$$\frac{t}{q_t} = \frac{1}{k_2 q_{e(theo)}^2} + \frac{t}{q_{e(theo)}} \qquad 9c$$

A plot of t/q_t versus t gives a slope and an intercept, from which the values of $q_{e\ (theo)}$(mg/g), and the pseudo- second order rate constant k_2 ($gmg^{-1}min^{-1}$), can be calculated respectively.

At time 0, the initial rate denoted as h_0 is given as

$$h_0 = k_2 C_0^2 \ldots\ldots\ldots\ldots\ldots\ldots\ldots\ldots\ldots\ldots\ldots\ldots 9d$$

where C_0 is the initial concentration before adsorption. h_0 is then evaluated from already determined k_2

Intra-particle diffusion model

The intra-particle diffusion model is based on the theory proposed by Weber and Morris. According to this theory,

$$q_t = k_{id} t^{0.5} + C \qquad 10$$

Where q_t is adsorption capacity at time t, k_{id} is intra-particle diffusion rate constant in $mg/g/min^{1/2}$.

This model shows whether the rate determining step is by the boundary film diffusion or by intra-particle diffusion.

Thermodynamic studies.

With all other parameter kept constant, adsorption experiments were carried out at temperatures of 50°C, 70°C and 90°C. To gain a better understanding of the adsorption mechanism, the thermodynamic parameters such as Gibb's free energy changes (ΔG), enthalpy change (ΔH), and entropy change(ΔS) were determined. Gibb's free energy of adsorption was computed from the equation (Han et al., 2010)]:

$$\Delta G = -RT\ln K_C \qquad 11$$

where ΔG is standard free energy change, R is universal gas constant(8.314 J/mol/ K), T is absolute temperature in K, and K_C is the equilibrium constant K_C, is defined as:

$$K_c = \frac{q}{C} \qquad 12$$

Where q is the concentration of adsorbed metal in mg/l, C is concentration in mg/l of Pb^{2+} solution after adsorption.

The values of ΔH and ΔS are then estimated from the relationship

$$\Delta G = \Delta H - T\Delta S \ldots\ldots\ldots\ldots\ldots\ldots\ldots\ldots 13$$

Results and discussion

Characterization of the adsorbents

Fourier Transform Infrared Spectroscopy (FT-IR) studies identify the functional groups in the4000–400 nm range. The spectra obtained are shown in Fig. 1(a) and (b). The spectra indicated a number of absorption peaks showing the complex nature of cattle bone. The functional group is one of the keys to understand the mechanism of metal binding on cattle bone [Wang et al., 2010]. There are several functional groups present and their wave numbers and absorption intensities before and after adsorption are shown on Table 1. The peak at 3379.1 cm^{-1} was assigned to OH group of hydroxyapatite mineral and NH group of collagen protein[Lurtwitayapont and Srisatit, 2010]. This shifted to 3442.92 cm^{-1} after adsorption with an intensity change of 22.8. The peak at 2919.04cm^{-1} of C-C of alkyl group shifted to 2918.25 cm^{-1} with an intensity change of 3.0066. C=O peak of collagen protein at 1541.04cm^{-1}[Lurtwitayapont and Srisatit, 2010] shifted slightly to 1541.31 cm^{-1} with an intensity change of 7.953. PO_4^{3-} of the hydroxyapatite mineral ($Ca_5(PO_4)_3OH$) of bones showed a peak at 1031.35cm^{-1}, which shifted to 1030.88$cm^{-1}$with an intensity change of 12.221. Carbonate CO_3^{2-}at 870.73cm^{-1} [Lurtwitayapont and Srisatit, 2010] shifted to 871.27 and had an intensity change of 19.029. A broad and strong band of Ca^{2+} at 561.79 cm^{-1} shifted to 562.71 cm^{-1} with an intensity change of 10.315. The observed changes in peaks and intensities are indications that interactions leading to adsorption actually occurred. Intensity changes at PO_4^{3-} and CO_3^{2-} peaks were noticeably much higher than those of other peaks, showing that more of the interactions and hence adsorption must have taken place in them.

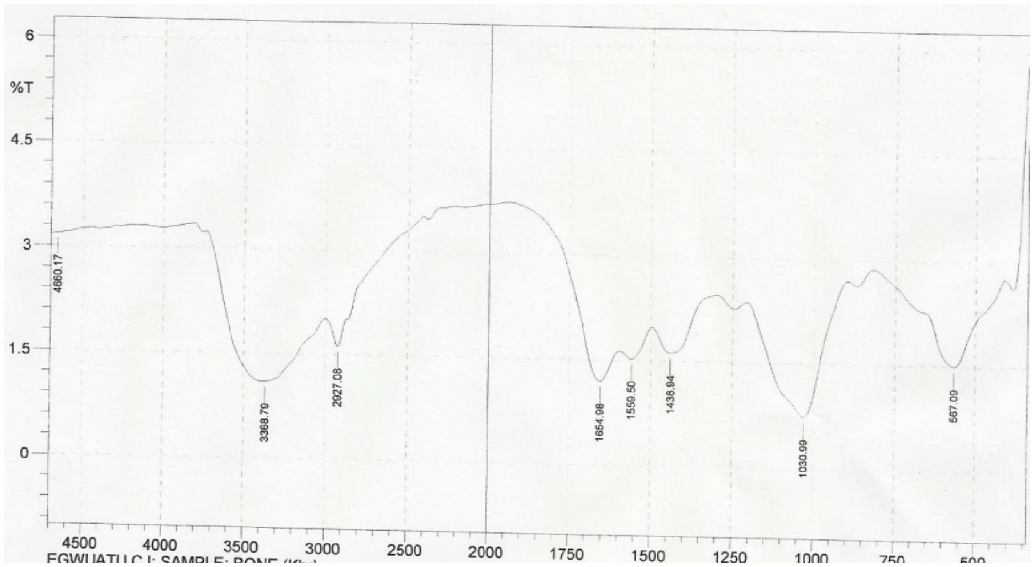

Figure 1a. IR spectrum of bone before adsorption

Table 2: IR data of cattle bone

Wavenumber(cm^{-1})		Intensity		Δ in intensity	Assigned functional groups
Pre-sorption	Post-sorption	Pre-sorption	Post-sorption		
3379.1	3442.92	-0.0046	0.224	0.2286	OH, NH, groups
2919.04	2918.23	0.0664	3.073	3.0066	C-C of alkyl group
1541.08	1541.31	0.255	8.208	7.953	C=O carbonyl group
1031.35	1030.88	0.437	12.658	12.221	PO_4^{3-} band
870.73	871.27	1.618	20.639	19.029	CO_3^{2-} band
561.79	562.71	0.682	10.997	10.315	Ca^{2+} band

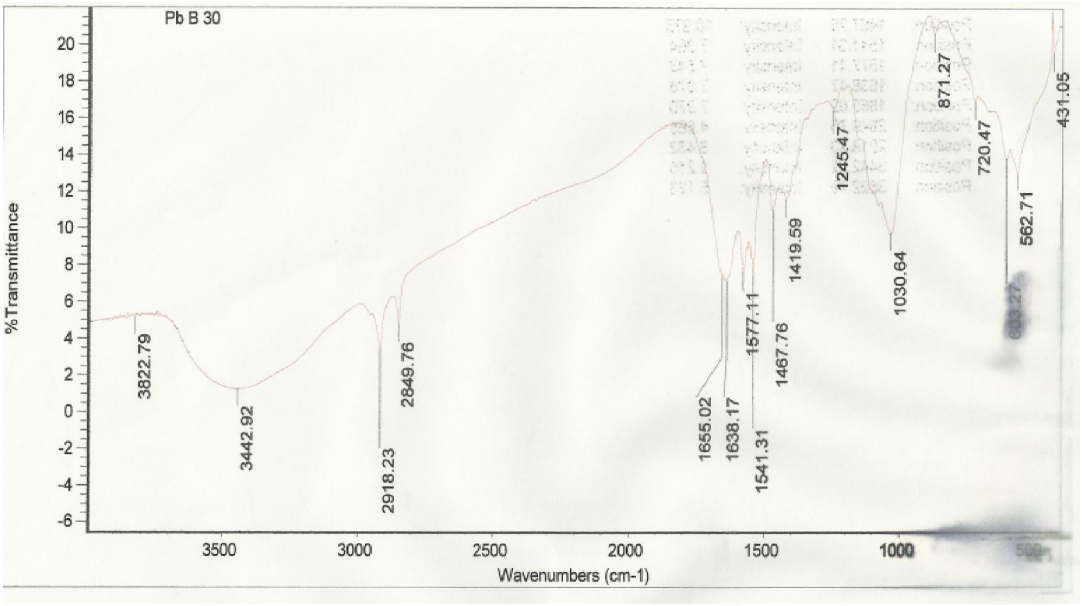

Figure 1b. IR spectrum of bone after adsorption

The effect of pH

Fig 2 shows the effect of pH on adsorption of Pb^{2+}. The pH for the optimum adsorption of Pb^{2+} on cattle bone is between 4 and 5. Adsorption was at its lowest at low pH. The effect of pH on Pb^{2+} removal can be explained considering the surface charge on the adsorbent material. At pH lower than 4 (low pH), the less adsorption was due to the high concentration of hydrogen ions. Hydrogen ions have the highest mobility ($36.25*10^{8}m^{2}s^{-1}V^{-1}$) of all the cations [Mortimer, 2008]; hence they would reach the adsorption sites faster than other cations. It then follows that at low pH, the functional groups available on the adsorbents surface are highly protonated resulting in repulsion between them and the positive lead ion during uptake and hence less adsorption of the preferred cations. With increasing pH, electrostatic repulsion decreases due to reduction of positive charge density of proton on the sorption sites thus resulting in enhancement of metal adsorption. Similar observations were reported by earlier researchers[Abasi et al., 2011].Further increase of pH above 6, led to a decrease in percentage adsorption. At this stage, the hydroxyl ions concentration has increased tremendously. This in effect resulted in lower removal efficiency.

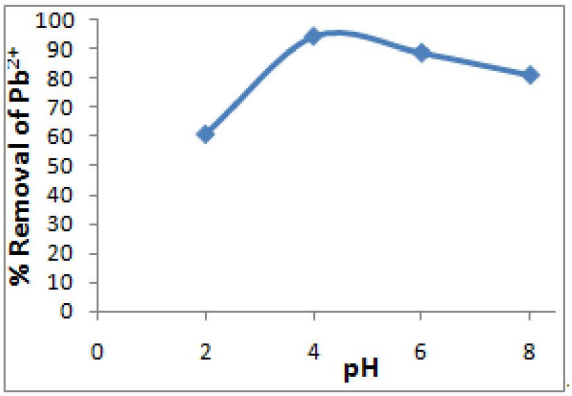

Figure 2. Effect of pH on the removal of lead ions

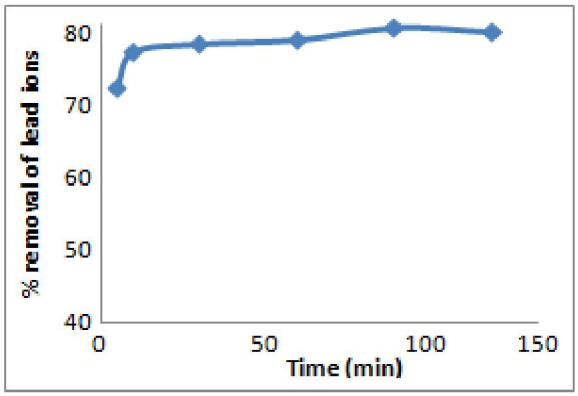

Figure 4. Effect of contact time on the adsorption lead ion

Effect of time

The first five minutes saw the removal of 72% of lead ions from the solution. As time progressed, less adsorption occurred as a result of saturation of lead ions on available sorption sites with lead ion. Equilibrium and maximum sorption of 80.5% occurred at 90min.

Effect of initial concentration

Percentage adsorption increased from 92 at concentration of 10mg/l to 94 at 30mg/l. Increase in concentration to 40 and 50mg/l gave sorption percentages almost the same with that at 30mg/l. At this point almost all the available sorption sites had been occupied and equilibrium almost attained.

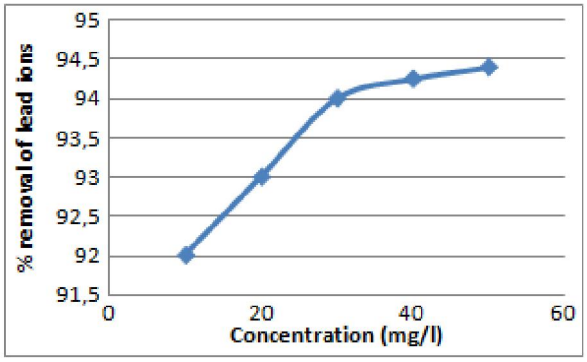

Figure 3. Effect of initial concentration on the removal of lead ion

Equilibrium studies See Appendix for this Part

Table 2 shows the isotherm parameters of lead ion adsorption. Correlation coefficient R^2 determines the fitness of models for experimental data. The higher the R^2 value, the better the model. Hence the fitness is as follows: Freundlich > Langmuir > Temkin > D.R. Better fitness for Freundlich model indicates a multilayer or heterogeneous adsorption. This could be due to complexity of structure and composition of the adsorbent. Better fitness for Langmuir model shows a monolayer adsorption indicating a homogeneous distribution on the sorbent surface, with negligible interaction between adsorbed molecules (Abasi et al., 2011) and also involving non dissociation of adsorbed molecules (Mortimer, 2008). Sorption intensity n was less than 1. Dimensionless separation factor R_L obtained from the Langmuir model was less than 1showing a favourable adsorption. The significance of R_L values is shown on table 1 (Momčilović et al., 2011). The Langmuir and Freundlich isotherms do not give any idea about adsorption mechanisms. However the magnitude of the mean sorption energy E_m determined from the D–R isotherm can be used for estimating the type of adsorption. It tells whether sorption occurs through physiosorption, ion exchange or chemisorption process. E_m values below 8kJ/mol show a physiosorption process involving forces like London dispersion forces, dipole–dipole attractions, and so on[Mortimer, (2008)]. E_m values between 8kJ/mol and 16kJ/mol indicate ion exchange mechanism, while that above 16kJ/mol indicates a chemisorption process. In chemical adsorption covalent bonds are formed between the atoms or molecules of the surface and the atoms or molecules of the adsorbed substance. E_m for lead adsorption was 91.287kJ/mol, indicating a chemisorption process.

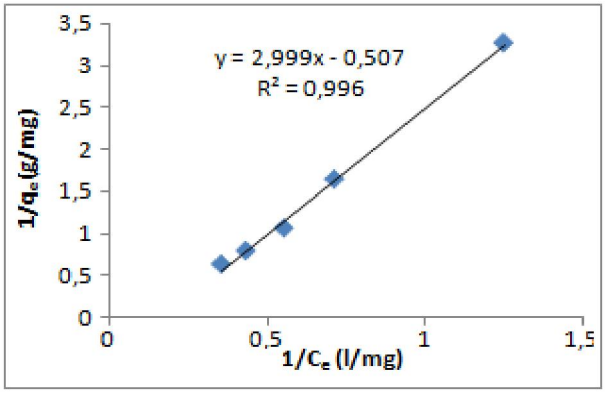

Figure 5. Langmuir isotherm for lead ion adsorption

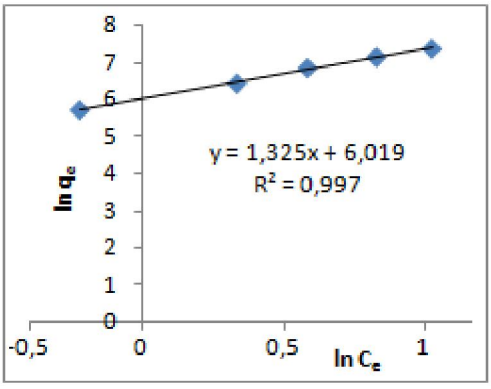

Figure 6. Freundlich isotherm for lead ion adsorption

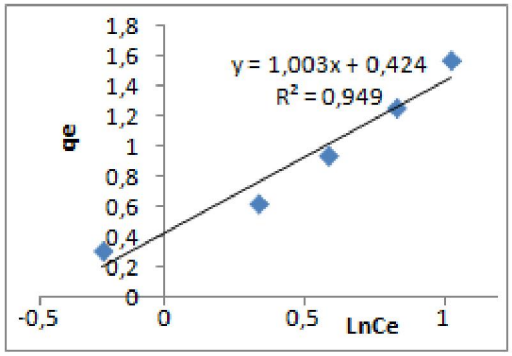

Figure 7. Temkin isotherm for lead ion adsorption

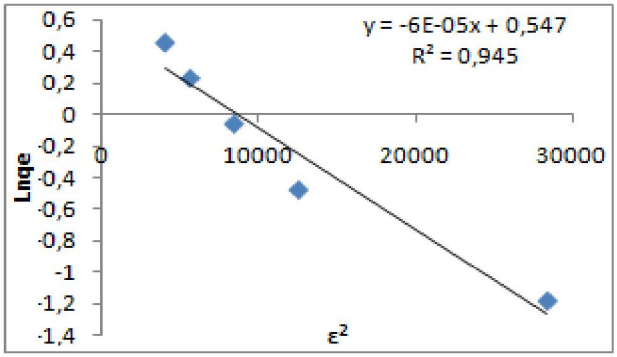

Figure 8. D-R isotherm for lead ion adsorption

Table 4: Isotherm parameters of lead ion adsorption

Parameters	**Model** Freundlich	Langmuir	Temkin	D-R
R^2	0.9975	0.9967	0.9499	0.9458
Q_m(mg/g)		1.95733		1.7287
N	0.7542			
K_F, K_L and K_T	0.411519	0.1705	1.5270	
R_L		0.369679		
B				0.00006
E(kJ/mol)				91.287

Kinetic Studies

Tables 3 shows results obtained for the kinetic parameters using Lagergren first order and pseudo – second order kinetic models. Experimental data fitted better into the pseudo-second order model, which gave higher coefficient of correlation (R^2) value than the Lagergren first order kinetic model. The rate constants k and initial rates of adsorption h_0 were determined from the pseudo-second order kinetics. Theoretical q_e obtained from the second order model (0.9695mg.g), was closer to that obtained from experiment (0.9667mg/g) than that obtained from first order model (0.0745mg/g). This suggests that the kinetics of lead adsorption onto cattle bone is more suitably described by the second order model than the first order model.

Table 3: Kinetic parameters

Kinetic Model	Pseudo 1st order	Pseudo 2nd order
R^2	0.8882	0.9999
$q_{e(exp)}$ (mg/g)	0.9667	
$qe_{(theo)}$(mg/g)	0.0745	0.9696
K_{ad}(g/mg/min)	0.0261	1.3119
h_o(gmg/l^2/min		1.2332

Intra particle diffusion

Fig.11. represents the plot of q_t versus $t^{1/2}$ for intraparticle transport of lead ion. The values of k_{id}, and C_i obtained for the plots are 0.0088mg/g/$min^{1/2}$ and 0.8771mg/g respectively. Values of C_i give an idea about the thickness of boundary layer. The larger the intercept, the greater the boundary layer effect [Li et al., 2010]. If the Weber–Morris plot of qt versus $t^{\frac{1}{2}}$ is linear and passes through the origin, then the sorption process is controlled only by intra-particle diffusion. However, for lead adsorption onto cattle bone, the data showed a multi-linear plot. This indicates that two or more steps were involved in the sorption process. The first, sharp portion has a very high slope indicating a high rate of sorption. This is attributed to the availability of active sorption sites at the initial stage. The second section has a gradient lower than the first, because less lead ions were sorbed in a longer time than at any other stage in the course of adsorption. The second linear portion was the gradual adsorption stage where intra-particle diffusion is the rate limiting step. Referring to Figure 11, none of the linear lines passed

through the origin. This indicated that intraparticle diffusion was not the only rate-limiting step in the sorption process (Wu et al., 2005).

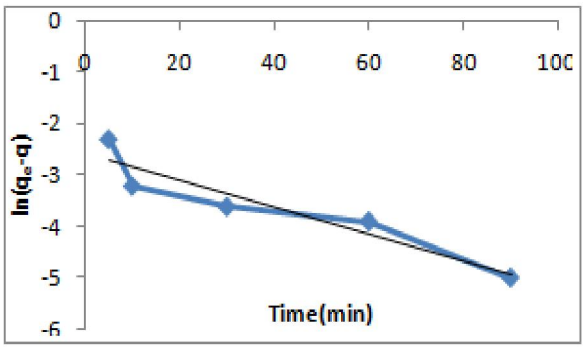

Figure 9. Langergren pseudo first order kinetic plot for lead ion adsorption

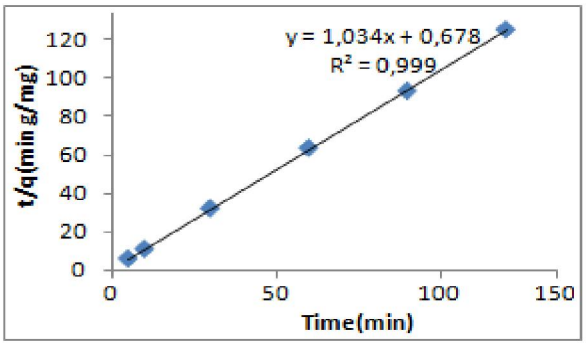

Figure 10. Pseudo second order kinetic plot for lead ion adsorption

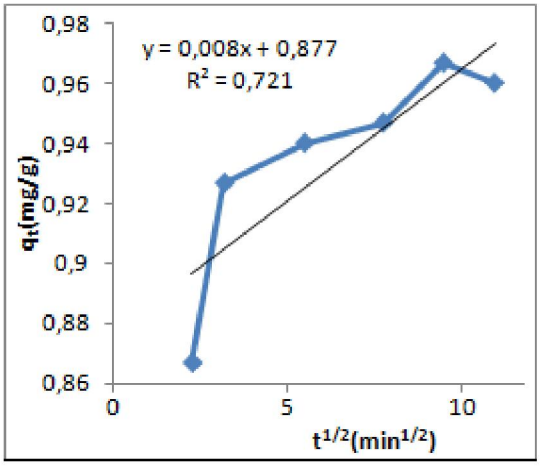

Figure 11. Weber-Morris plot for lead ion adsorption

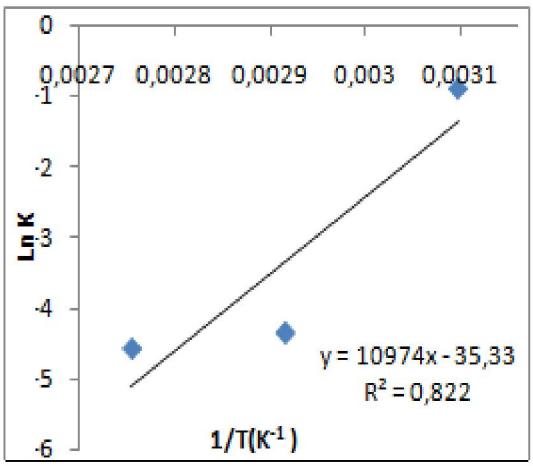

Figure 12: van't Hoff plot for adsorption of lead ion

Thermodynamic study

The thermodynamic parameters are given in Table 4. Equilibrium constant K_c for the adsorption of Pb^{2+} on cattle bone, increased with increase in temperature. Equilibrium in these cases shifted to the right resulting to increased adsorption. ΔG was found to be positive. The positive values of ΔG increased with the rise in temperature. Positive values of ΔG indicate an endergonic process i.e. processes that are non-spontaneous and less feasible process while negative values indicate an exergonic process i.e. processes that are spontaneous and feasible (Gerc & Gerc, 2007). Enthalpy change ΔH was positive. Positive values of ΔH indicate endothermicity while negative values indicate exothermicity of adsorption process. Entropy change ΔS was found to be negative which shows a decrease in degree of randomness (Nuhoglu & Malkoc, 2009).

Table 4.Thermodynamic parameters

Temperature (K)	323	343	363
Equilibrium constant	2.42	77	96.5
ΔH(KJ)	91.237		
ΔS(KJ/mol/K)	-0.294		
ΔG(KJ/mol)	186.13	192	197.88

Conclusion

The present work explored a new cheaper and more economical biosorbent from cattle bone as an alternative to costly adsorbents for the removal lead ions. The main advantages include its availability, low cost (inexpensive), effectiveness and sorption capability. . This work shows that

- the sorption process was affected by experimental conditions such as initial metal concentration, pH and contact time.
- the pH for optimum sorption capacity is 4
- sorption was endothermic, non-spontaneous and less feasible
- second order kinetic model best described the sorption process
- Sorption was by chemisorption process

Reference

Abasi CY, Abia AA, Igwe JC, (2011) Adsorption of lead II and Cadmium II ions by unmodified Raphia Palm (*RaphiaHookeri*) fruit endocarp. *Environ. Res. J,* **5**, 104-113.

Abdelwahab O, (2007) Kinetics and isotherm studies of copper II removal from wastewater using various adsorbents. *Egypt J. Aquatic*. Res. **33,** 125–143.

AjayKumar AV, Darrwish NA, Hilal N, (2009) Study of various parameters in the biosorption of heavy metals on activated sludge. *World Appl. Sci. J.* 5 (SpecialIssue for Environment), 32–40.

Bennett MC, Abram JC, (1967) Adsorption from solution on the carbon and hydroxyapatite components of bone char. *J. Colloid Interf. Sci.* 23, 513–521.

Bergeson LL,(2008) "The proposed lead NAAQS: Is consideration of cost in the clean air act's future? *Environmental Quality Management* **18**, 79.

Bertazzo S, Bertran CA (2006)Morphological and dimensional characteristics of bone mineral crystals. *Bioceramics* (Pt. 1 2), 3–10.

Boskey A, Pleshko Camacho N (2007) FT-IR Imaging of Native and Tissue-Engineered Bone and Cartilage. *Biomaterial*s 28(15), 2465–2478.

Cheung WH, Szeto YS, McKay G (2007) Intraparticle diffusion processes during acid dye adsorption onto chitosan. *Bioresour.Technol*. 98, 2897–2904.

Christoffersen J, Christoffersen MR, Larsen R, Moller IJ (1991) Regeneration by surface-coating of bone char used for defluoridation of water. *Water Res*. 25, 227–229.

Freundlich H (1906) Adsorption in solution. Phys. Chem. Soc. 40, 1361-1368.

Gerc el Ö Gerc el HF (2007) Adsorption of lead(II) ions from aqueous solutions by activated carbon prepared from biomass plant material of *Euphorbia rigida*. *Chem. Eng. J.* 132289–297

Ghodbane I, Nouri L, Hamdaoui O, Chiha M (2008) Kinetic and equilibrium studyfor the sorption of cadmium(II) ions from aqueous phase by eucalyptus bark. *J.Hazard. Mater.* 152 (1),148–158.

GolubMS ed. (2005). "Summary". Metals fertility and reproductive toxicity. Taylor and Francis, Boca Raton Fla.:

Gu B, Liang L, Dickey MJ, Yin X, Dai S (1998) Reductive precipitation of uranium (VI) by zero-valent iron. *Environ. Sci. Technol.* 32, 3366–3373.

Han RP, Zhang LJ, Song C, Zhang MM, Zhu HM, Zhang LJ (2010) Characterization of modified wheat straw kinetic and equilibrium study about copper ion and methylene blue adsorption in batch mode. *Carbohydrate Polymer* 79, 1140–1149.

Ho YS, McKay G, Wase DAJ, Foster CF (2000) Study of the sorption of divalent metal ions on to peat. *Ads. Sci. Technol.* 18, 639–650.

Horsfall Jr . M, SpiffAI, Abia AA (2004) Studies on the influence ofmercaptoacetic acid (MAA) modification of cassava (*Manihot esculenta Cranz*) waste biomass on the adsorption of $Cu^{2+}$and$Cd^{2+}$from aqueous solution. *Bull Korean. Chem. Soc*. **25,** 969–976.

http://www.pencils.com/pencil-history. Retrieved 7, April 2007.].

Igwe JC, Abia AA (2007)Equilibrium sorption isotherm studies of Cd(II)Pb(II) and Zn(II) ions detoxification from waste water usingunmodified and EDTA-modified maize husk. Electron. *J. Biotechnol*. **10,** 536–548.

Krika F, Azzouz N, Chaker Ncibi M(2012) Adsorptive removal of cadmium from aqueous solution by cork biomass: Equilibriumdynamic and thermodynamic studies. *Arabian Journal of Chemistry* doi:10.1016/j.arabjc.2011.12.013

Langmuir I(1918) The adsorption of gases on plane surfaces of glass mica and platinum. *J. Am. Chem. Soc.* 40, 1361–1368.

Larsen MJ, Pearce EIF, Jensen SJ (1993) Defluoridationof water at high pH with use of brushite, calcium hydroxide and bone char. *J. Dental Res.* 72, 1519–1525.

Li Y, Dua Q, Wangb X, Zhanga P, WangbD, Wanga Z, Xia Y (2010) Removal of lead from aqueous solution by activated carbon prepared from *Enteromorpha prolifera* by zinc chloride activation. *J. Hazard.Mater*. 183, 583-589.

Lurtwitayapont S, Srisatit T (2010) Comparison of Lead Removal by Various types of Swine Bone Adsorbents. *Environment Asia* 3(1), 32-38.

Mahamadi C, Nharingo T (2010) Utilization of water hyacinth weed(*Eichhornia crassipes*) for the removal of Pb(II) Cd(II) and Zn(II) from aquatic environments: An adsorption isotherm study. *Environ. Technol*. 31,1221–1228.

Momčilović M, Purenović M, Bojić A, Zarubica A, Ranđelović M (2011). Removal of lead(II) ions from aqueous solutions by adsorption onto pine cone activated carbon. *Desalination* 27, 653–59.

Mortimer RG (2008) PhysicalChemistry 3ed. Elsevier Academic Press. London.

Nuhoglu Y Malkoc E (2009) Thermodynamic and kinetic studies for environmentally friendly Ni(II) biosorption using waste pomace of olive oil factory. *Bioresour. Technol*. 100 2375–2380 .

Pehlivan E, Yanik BH, Ahmetli G, Pehlivan M (2008) Equilibrium isotherm studiesfor the uptake of cadmium and lead ions onto sugar beet pulp. *Bioresour.Technol*. 99, 3520–3527.

Phantumvanit P, LeGeros RZ (1997) Characteristics of bone char related to efficacy of fluoride removal form highly fluoridated water. *Fluoride* 30, 207–218.

Sameer AI -A Fawzi B Fadel M (1999)Sorption of copper andnickel by spent animal bones. *Chemosphere* 39(12) 2087-96.

Sari A, Tuzen M (2009) Kinetic and equilibrium studies of biosorption of Pb(II) and Cd(II) from aqueous solution by macrofungus (*Amanita rubescens*) biomass. *J. Hazard. Mater*. 1641004–1011.

Vijayaraghavan K, Padmesh TVN, Palanivelu K, Velan M (2006) Biosorption of nickel(II) ions onto *Sargassumwightii*: application of two-parameter and three-parameter isotherm models. *J. Hazard Mater*. 133, 304–308.

Vimala R, Das N(2009) Biosorption of cadmium(II) and lead(II) from aqueous solutionsby using mushrooms: a comparative study. *J. Hazard. Mater*. 168, 376–382.

Wang X, Zhu N, Yin B (2008)Preparation of sludge-based activated carbon and its application in dye wastewater treatment. *J. Hazard. Mater*. 153, 22-27.

Wang XJ, Xia SQ, Chen L, Zhao JF, Chovelon JM, Nicole JR (2006) Biosorption of cadmium (II) and lead (II) ions from aqueous solutions onto dried activated sludge. *J. Environ. Sci*. 18, 840-844.

Weber WJ, Morris JC (1963) Kinetics of adsorption on carbon from solution . *J. Sanit. Eng. Div. Am. Soc. Civ. Eng*. 89, 31–60.

Wu FC, Tseng RS, (2005) Comparisons of porous and adsorption properties of carbons activated by steam and KOH. *J. Colloid Interface Sci*. 283, 49–56.